Published in final edited form as:
Mol Imaging Biol. 2010 ; 12(1): . doi:10.1007/s11307-009-0240-1.

Bioluminescence Imaging in Mouse Models Quantifies β Cell Mass in the Pancreas and After Islet Transplantation

John Virostko[1,2], **Aramandla Radhika**[3], **Greg Poffenberger**[3], **Zhongyi Chen**[3], **Marcela Brissova**[3], **Joshua Gilchrist**[3], **Brian Coleman**[3], **Maureen Gannon**[3,4,5], **E. Duco Jansen**[2], and **Alvin C. Powers**[3,4,6]

[1]Vanderbilt University Institute of Imaging Science, Nashville, TN, USA

[2]Department of Biomedical Engineering, Vanderbilt University, Nashville, TN, USA

[3]Department of Medicine, Division of Diabetes, Endocrinology, and Metabolism, Vanderbilt University, Nashville, TN, USA

[4]Department of Molecular Physiology and Biophysics, Vanderbilt University, Nashville, TN, USA

[5]Department of Cell and Developmental Biology, Vanderbilt University, Nashville, TN, USA

[6]VA Tennessee Valley Healthcare System, Nashville, TN, USA

Abstract

Purpose—We developed a mouse model that enables non-invasive assessment of changes in β cell mass.

Procedures—We generated a transgenic mouse expressing luciferase under control of the mouse insulin I promoter [mouse insulin promoter-luciferase-Vanderbilt University (MIP-Luc-VU)] and characterized this model in mice with increased or decreased β cell mass and after islet transplantation.

Results—Streptozotocin-induced, diabetic MIP-Luc-VU mice had a progressive decline in bioluminescence that correlated with a decrease in β cell mass. MIP-Luc-VU animals fed a high-fat diet displayed a progressive increase in bioluminescence that reflected an increase in β cell mass. MIP-Luc-VU islets transplanted beneath the renal capsule or into the liver emitted bioluminescence proportional to the number of islets transplanted and could be imaged for more than a year.

Conclusions—Bioluminescence in the MIP-Luc-VU mouse model is proportional to β cell mass in the setting of increased and decreased β cell mass and after transplantation.

Keywords

Bioluminescence imaging; Luciferase; Beta cell; Pancreatic islet; Transplantation; Optical imaging; Islet mass; Beta cell mass; Imaging

Correspondence to: Alvin C. Powers, al.powers@vanderbilt.edu.
Virostko and Radhika contributed equally to this manuscript.

Electronic supplementary material The online version of this article (doi:10.1007/s11307-009-0240-1) contains supplementary material, which is available to authorized users.

Introduction

Studies of the complex dynamics of β cell loss in the pre-diabetic and diabetic state are hindered by the inability to non-invasively assess pancreatic β cell mass. Non-invasive imaging capabilities may also aid the development of therapeutic interventions intended to slow or halt diabetes-related β cell loss, to regenerate islets or increase islet mass, and to improve β cell survival post islet transplantation [1, 2]. β cell mass is most commonly estimated from measurements of insulin secretion [3] or morphometric analysis of histological sections [4, 5]. However, metabolic assessments reflect aspects of β cell function rather than mass; the two metrics do not necessarily correlate, especially in pathological diabetic states. For instance, fasting hyperglycemia typically presents only after β cell mass has been reduced by over 50% [6–9]. Morphometric analysis requires sacrificing the animal, obviating sequential studies in the same animal.

From the perspective of imaging physics, the pancreatic β cell is a problematic candidate for imaging by currently available modalities [10]. Pancreatic islets are small and are distributed sparsely throughout the pancreas, constituting only 1–2% of the total pancreatic mass. In addition, islets possess no known intrinsic contrast from the surrounding exocrine pancreas [10–12]. Studies seeking to specifically image and quantify the β cell rather than the entire islet are further complicated by the fact that the β cell comprises only one of five major islet endocrine cell types. Recent international workshops have focused on overcoming the difficulties in imaging the β cell and spurring development of novel islet imaging techniques [12]. A variety of modalities, including magnetic resonance imaging (MRI), positron emission tomography (PET), and optical imaging have now been applied in attempts to image pancreatic islets [10]. Efforts using MRI are focusing largely on labeling islets *in vitro* with MRI contrast agents prior to transplantation [13–19]. PET imaging of islets has also used *in vitro* islet labeling techniques [20–22] as well as radioligands targeted to the β cell [23–28]. While promising, none of these imaging modalities have been shown to reflect β cell mass in states of increased and decreased β cell mass and following islet transplantation.

Bioluminescence imaging (BLI) provides a means of imaging gene expression non-invasively using an optical reporter gene [29]. Initial attempts to apply BLI to islet imaging employed viral transduction of a vector encoding luciferase cDNA to label isolated islets [30–32]. This strategy proved valuable for studies of transplanted islets, revealing a linear relationship between bioluminescence emission and islet mass that could be tracked repeatedly and non-invasively for several months post-transplantation [31–33]. While the current studies were underway, two transgenic mouse lines expressing the luciferase optical reporter under control of insulin promoter fragments have been reported [34, 35]. These mice have been used to track pancreatic islet bioluminescence in animal models of diabetes and transplantation but have several limitations. A transgenic line expressing luciferase under the rat insulin promoter suffered from genomic imprinting of the transgene, gender-related dissimilarity in BLI, extra-pancreatic luciferase expression, and variability in the amount of light emitted between littermates [35]. These limitations make it challenging to use this transgenic line to reproducibly assess β cell mass, since all mice in this line do not exhibit similar BLI. Park and colleagues expressed luciferase in β cells using the same fragment of the mouse insulin I promoter used in the present report and showed that BLI originated from beta cells, but did not examine whether BLI reflected β cell mass [34]. In this report, we describe the development and characterization of a trans-genic mouse model [mouse insulin promoter-luciferase-Vanderbilt University (MIP-Luc-VU)] which expresses luciferase under the control of the mouse insulin promoter. We have utilized this model to demonstrate that bioluminescence emission is indicative of increased or decreased β cell mass in the pancreas and β cell mass following islet transplantation.

Materials and Methods

Generation of Transgenic Mouse Line

We generated transgenic mice expressing the luciferase optical reporter cDNA *Luc* under control of the 9.2 kb mouse insulin I promoter (MIP), which was graciously provided by Mark Magnu-son at Vanderbilt University [36]. The luciferase cDNA was released from the BlueScript vector (Stratagene, La Jolla, CA) by digestion with *KpnI* and *NotI*, purified by agarose gel electrophoresis, and subcloned into a vector containing the MIP fragment and intronic and poly A sequences from the rabbit beta globin gene. The purified DNA was injected by the Vanderbilt University Transgenic/ES core into Friend leukemia Virus B strain (FVB/NJ, Jackson Labs, Bar Harbor, ME) mouse embryos. FVB mice, which have white fur, were chosen to limit absorption of photons emitted from the bioluminescence reaction. Four MIP-Luc-VU founder lines were generated and genotyped by Southern blot. *In vivo* bioluminescence imaging was subsequently used to phenotype the offspring of the founder lines, as previously described by Contag and co-workers [37]. From this screening, the founder line with the highest and most consistent luciferase expression over the pancreatic region was selected for further study. The transgene copy number was estimated to be three using Southern blot standardized to a known amount of DNA. The MIP-Luc-VU line has been submitted to the mouse collection of the Beta Cell Biology Consortium (http://www.betacell.org) and is available in The Jackson Laboratory Induced Mutant Resource Repository (Bar Harbor, Maine, USA) as Stock No. 007800 by searching the JAX Mice database (http://jaxmice.jax.org/query).

Using a similar approach, we also generated transgenic mice expressing luciferase under control of a 1.0 kb *Pst-Bst* fragment of the pancreatic-duodenal homeobox factor-1 promoter (*pdx1*-Luc) that was previously shown to drive transgene expression to all islet cells [38]. Five *pdx1*-Luc founder mice were genotyped by Southern blot and phenotyped by bioluminescence imaging. All experiments involving animal subjects were approved by The Vanderbilt University Institutional Animal Care and Use Committee.

Islet Isolation

Islets were isolated by dissection of the splenic portion of the pancreas and collagenase P digestion as previously described [39]. Islets were handpicked under microscopic guidance and washed three times with 10 mM phosphate-buffered saline containing 1% mouse serum and suspended in 30 μL of the same solution prior to transplantation. A cell perifusion system was used to test the response of isolated islet preparations to stimuli of 16.8 mM glucose, 16.8 mM glucose+100 μM isobutyl methyl xanthine, and 2.8 mM glucose+300 μM tolbutamide as described [40].

Diabetes Induction

MIP-Luc-VU mice (males, 8 weeks of age) were rendered diabetic by a single intraperitoneal injection of streptozotocin (STZ, 175 mg/kg in 0.1 M citrate buffer, pH4.5). Blood glucose measurements were obtained using tail vein blood measured with an Accu-chek glucose meter (Roche Diagnostics, Indianapolis, IN).

High-Fat Diet

MIP-Luc-VU mice (females, 8 weeks of age) were fed a high-fat diet consisting of 35.5% fat content, 36.3% carbohydrate, and 20.0% protein (Bio-Serv, Frenchtown, NJ) for 6 months. Food was administered *ad libitum* and changed twice a week.

Islet Transplantation

Nondiabetic, immunodeficient (non-obese diabetic-severe combined immunodeficiency (NOD-scid), Jackson Labs, Bar Harbor, ME) and FVB/NJ mice (8–12 weeks of age) were used as transplant recipients [39]. Islets obtained from MIP-Luc-VU mice were transplanted into the liver of host mice by injection into the portal venous system or beneath the renal capsule, as previously described [39].

Insulin Content

Pancreata, renal islet grafts, or livers containing islets were excised from anesthetized animals. Organs were cleaned of connective tissue, blotted dry, and weighed. Tissue was homogenized in acid alcohol (1 ml 12 M HCL/110 mL 95% ethanol) and incubated for 48 h at 4°C under mild agitation. The homogenate was centrifuged at 2,500 rpm for 30 min at 4°C. The supernatant was collected for radioimmunoassay and stored at −20°C. Insulin content was measured with a heterospecies-specific radioimmunoassay using antibody-coated tubes (ICN Diagnostics, Costa Mesa, CA) and I^{125}-human insulin (Diagnostic Products, Los Angeles, California), as previously described [41].

Immunocytochemistry

Dissected mouse pancreata were fixed, embedded, and sectioned using methods previously described [42]. Cryosections were incubated with primary antibodies overnight at 4°C. Guinea pig anti-insulin IgG (1:1,000), sheep anti-somatostatin IgG (1:500), and rabbit anti-glucagon IgG (1:10,000) were from Linco Research, Inc. (St. Charles, MO). Rabbit anti-luciferase (1:250) was obtained from Cortex Biochem, Inc. (San Leandro, CA). Secondary antibodies conjugated with Cy2, Cy3, or Cy5 fluorophores (1:1,000, Jackson ImmunoResearch Laboratories, Inc., West Grove, PA) were applied to the tissue sections for 1 h at room temperature.

To determine β cell mass and luciferase expression in the pancreas of MIP-Luc-VU mice, 7-μm thick pancreatic sections spaced by 250μm from three different levels of the pancreatic tissue block were stained and imaged using a ×2 and ×20 objective. Using MetaMorph v6.1 software (Universal Imaging, Downington, PA), integrated morphometry was used to calculate the relative pancreatic area of islet β cells and luciferase-expressing cells by dividing insulin and luciferase stained area, respectively, by the total pancreatic area, as previously described [41, 43]. The mass of β cells and luciferase-expressing cells was then determined by multiplying the relative area of each cell type by the total pancreatic weight.

Bioluminescence Imaging

All bioluminescence imaging (BLI) was performed using an IVIS 200 CCD camera (Xenogen/Caliper, Alameda, CA) as previously described [30, 31]. For studies performing BLI in vitro, islets were cultured overnight in RPMI with 10% FBS and 2.5, 5.6, 11.0, or 16.7 mM glucose. Islets were placed in a black well plate to prevent light scatter from adjacent wells (30 islets per well) and placed on the heated (37°C) imaging platform of the IVIS system. Thirty-five microLiters of the substrate D-luciferin (Promega, Madison, WI) at a concentration of 15 mg/ml was added to 500 μL of culture solution prior to imaging. Bioluminescence images were integrated for a period of 1 min. Images were taken immediately post-substrate addition to 5 min post-administration, in order to capture the peak in bioluminescence intensity, as previously described [31]. The luciferase activity of islet homogenates was measured by luminometer as described [31].

In vivo BLI was performed as previously described [30, 31]. Anesthesia was induced and maintained with isoflurane (1.5% in 98.5% O2). The substrate D-luciferin (at a concentration of 15 mg/ ml) was injected into the intraperitoneal cavity with a dose of 150

mg/kg. For imaging islets in the pancreas and islets transplanted to the kidney, animals were oriented laterally, with their left-side facing up toward the camera. For imaging islets transplanted to the liver, animals were placed in the supine orientation. To ensure peak bioluminescence was captured, animals were imaged up to 12 min post-injection, with peak luminescence typically reached approximately 10 min after luciferin administration. Bioluminescence images were integrated for 1 min. Bioluminescence intensity was quantified from the image of peak bioluminescence using Living Image analysis software (Xenogen, Alameda, CA). Equal area regions of interest (ROI) were centered over the bioluminescent region. Photon counting measurements summed bioluminescent intensity for all pixels within the ROI over the integration time.

Luminescent Bead Imaging

In order to quantify light attenuation in obese animals fed a high-fat diet, we employed constant intensity luminescent beads, as previously described [30, 31]. Immediately after sacrificing each animal on a high-fat and regular diet, we placed a luminescent bead in the anatomical region of the pancreas, closed the animal, and then imaged using the IVIS 200 CCD camera with a 10 s exposure. ROIs were drawn over the bead luminescence and photon counting measurements were performed to quantify light emission. The slope of the linear regression relating bead luminescence to body weight was used to normalize BLI measurements for obese animals fed a high-fat diet.

Three-Dimensional BLI Image Reconstruction

Three-dimensional reconstruction of in vivo bioluminescence was performed using the Living Image® Software 3D Analysis Package (Xenogen, Alameda, CA), as previously described [44, 45]. Briefly, the inverse diffusion model of light propagation was applied to spectrally-filtered bioluminescent image information to reconstruct the bioluminescent source location and intensity. Spectral imaging was obtained by imaging bioluminescence through six 20-nm bandpass filters at wavelengths from 560 to 660 nm. A structured light image was taken to reconstruct the surface topography of the mouse. Images were reconstructed using the optical properties of muscle tissue included with the software package.

Statistical Analysis

Unpaired *t* test and ANOVA were used to compare experimental results. Data are expressed as means±SEM.

Results

In Vivo Bioluminescence Imaging

After injection of the luciferin substrate into MIP-Luc-VU mice, bioluminescence was visible in an area consistent with the anatomical location of the pancreas in all four founder lines. We noted a small region of brain expression in two of the founder lines that were subsequently not used. We selected the founder line with the most consistent bioluminescence from the pancreas for further studies (Fig. 1). A bioluminescence image of the exposed pancreas indicated that all light was emanating from the pancreas (Fig. 1b). No emitted light was detected from other organs of the MIP-Luc-VU mouse. Three-dimensional reconstruction of bioluminescence from the pancreas of a MIP-Luc-VU mouse shows the anatomical location of bioluminescent islet clusters within the mouse volume (Fig. 1d). BLI in this founder line is similar in males and females, constant in subsequent generations of mice, and similar in mice of different ages (Fig. 1 legend).

After injection of luciferin into the transgenic mouse line expressing luciferase under control of the pdx-1 promoter fragment (*pdx1*-Luc), bioluminescence was detected from the entire animal with highest expression visible in areas of exposed skin (tail, paws, and nose) (Supplementary Figure 1). All five founder lines showed a similar pattern of bioluminescence throughout the animal, indicating that this *pdx1* promoter fragment has some expression in other tissues such as hair follicles [38]. Islets isolated from *pdx1*-Luc animals emitted light both *in vitro* and after transplantation to the renal capsule (Supplementary Figure 1). The luciferase content of *pdx1*-Luc islets was an order of magnitude lower than the luciferase content of MIP-Luc-VU islets. Since islets in the pancreas could not be distinguished over background expression by bioluminescence in the *pdx1*-Luc mice, these animals were not characterized further.

MIP-Luc-VU Islet Function is Normal

Functional testing of MIP-Luc-VU animals was performed to ensure that the transgenic expression of luciferase did not alter islet function. Intraperitoneal glucose tolerance testing of MIP-Luc-VU mice was similar to non-transgenic mice (Fig. 2a). Isolated MIP-Luc-VU islets displayed a similar response to the islet secretagogues glucose, isobutyl methyl xanthine, and tolbutamide as wild-type islets in a cell perifusion system (Fig. 2b). Repeated measures ANOVA verified no statistical difference in glucose-tolerance testing or islet perfusion testing between MIP-Luc-VU mice and non-transgenic mice. By immunocytochemistry, MIP-Luc-VU islets displayed the typical murine islet architecture: a core of β cells surrounded by a mantle of alpha and delta cells with approximately one quarter (23.6±1.3%) of β cells expressing luciferase. Luciferase expression was detected primarily in β cells (Fig. 2f). A small fraction of luciferase-expressing cells (0.93%) did not stain for insulin; these cells were also negative for glucagon and somatostatin. The fraction of β cells expressing luciferase was examined across several mice examined and was similar in successive generations of MIP-Luc-VU mice.

In Vitro Bioluminescence Imaging of MIP-Luc-VU Islets

In order to determine the relationship between the number of islets and the bioluminescence emission, increasing numbers of islets isolated from MIP-Luc-VU mice were placed in 24-well plates. After addition of luciferin to the culture media, MIP-Luc-VU islets, but not control islets, emitted bioluminescence, which could be detected in individual islets and islet clusters by a CCD camera (Fig. 3). BLI correlated with the number of islets in each well (Fig. 3). The luciferase activity in islet lysates similarly correlated with the number of islets (Fig. 3). As previously shown by our group, control wild-type islets do not emit bioluminescence [31].

BLI Quantifies β Cell Mass in a Model with Decreased β Cell Mass

Following the injection of streptozotocin (STZ) into MIP-Luc-VU mice, there was a successive decline in bioluminescence intensity (Fig. 4a). By the eighth day after STZ treatment, BLI values had fallen by 78% (from $3.29\pm0.31\times10^6$ to $0.74\pm0.09\times10^6$photons/s) while blood glucose levels rose from normal values (147±8 mg/dl) to more than 500 mg/dl (Fig. 4a). The luciferase activity of extracted pancreata from MIP-Luc-VU mice 8 days after STZ injection was reduced 84% compared with the luciferase activity of untreated MIP-Luc-VU mice ($0.62\pm0.01\times10^5$ versus $3.96\pm0.28\times10^5$RLU/g pancreas weight, respectively; Fig. 4b). The pancreatic insulin content of MIP-Luc-VU mice 8 days after STZ treatment decreased by 96% compared with untreated controls (1.81±0.35 versus 49.83± 1.94 μg protein/g pancreas weight; Fig. 4b).

Immunocytochemistry of STZ-treated MIP-Luc-VU pan-creata demonstrated a marked reduction in insulin-stained area (Fig. 4c). Morphometric analysis indicated that 8 days after

STZ treatment there was a 93% decrease in β cell mass versus untreated controls (Fig. 4d). There was a proportional decline in luciferase-expressing cell mass as well. Before and after STZ treatment there was maintenance of the ratio of approximately one quarter (29.4±1.4%) of β cells expressing luciferase.

Bioluminescence imaging was performed on MIP-Luc-VU mice during intraperitoneal glucose-tolerance testing to determine the effect of transient hyperglycemia *in vivo*. Bioluminescence imaging performed 30 min after glucose bolus, at the point of highest blood glucose, was not different than bioluminescence measurements at normal blood glucose levels (data not shown). To further investigate the effect of glucose on bioluminescence, isolated MIP-Luc-VU islets cultured overnight in increasing glucose concentrations exhibited greater bioluminescence and luciferase activity (Supplementary Figure 2).

BLI Quantifies β Cell Mass in a Model with Increased β Cell Mass

MIP-Luc-VU animals fed a high-fat diet exhibited a gradual increase in body weight over littermates fed a regular diet (Fig. 5a). After 6 months on a high-fat diet, bioluminescence emission from MIP-Luc-VU animals was nearly twice that of animals on a regular diet ($5.68\pm0.51\times10^6$ versus $2.87\pm 0.38\times10^6$photons/s for control animals; Fig. 5b). We have previously described that the location of the bioluminescent source affects BLI [30]. To investigate whether the increased body mass of animals on the high-fat diet affected bioluminescence measurements via increased light attenuation by fat and tissue overlying the pancreas, we used constant light-emitting beads to assess the extent of this effect. These beads provide a constant light source surrogate for BLI, permitting studies of factors influencing BLI measurements. As Fig. 5c illustrates, obese animals on a high-fat diet exhibited lower light emission from these beads than animals on a regular diet. Bead luminescence correlated inversely with animal weight (r^2=0.5732), indicating light attenuation in the obese animals (Fig. 5d). Immunohisto-chemistry of animals on the high-fat diet revealed increased islet size compared with animals fed a regular diet (Fig. 5e). Bioluminescence measurements normalized for the increased light attenuation in obese animals fed the high-fat diet (as assessed using the constant light beads) correlated with β cell mass (Fig. 5f). Animals fed the high-fat diet exhibited a blunted response to a glucose bolus during intraperitoneal glucose-tolerance testing (Supplementary Figure 3).

In Vivo Imaging of Transplanted Islets

MIP-Luc-VU islets transplanted beneath the renal capsule (Fig. 6a) or into the liver via the portal vein (Fig. 6b) of NOD-scid mice were visible in the expected anatomical location. One hundred MIP-Luc-VU islets transplanted beneath the renal capsule of one FVB host continued to emit bioluminescence up to 16 months after transplantation (Supplementary Figure 4). Three-dimensional reconstruction of the BLI of transplanted islets demonstrated that islets transplanted beneath the renal capsule were in a compact, contiguous location (Fig. 6c), whereas islets transplanted via the portal vein were dispersed and scattered throughout the liver (Fig. 6d). We have noticed that the BLI of intrahepatic islets is usually not uniformly distributed over the liver region, indicating that after portal vein injection, islets do not flow into all lobes of the liver equally.

MIP-Luc-VU islets transplanted beneath the kidney capsule of NOD-scid mice revealed a linear relationship between the number of islets transplanted and bioluminescence (r^2 =0.7922; Fig. 6e). Grafts were subsequently excised and assayed for insulin content, which correlated linearly with the number of islets (r^2 =0.8143). Islets transplanted to the liver of NOD-scid mice also showed a linear relationship between bioluminescence and the number of islets transplanted (r^2=0.5481) and between the hepatic insulin content and number of

islets transplanted ($r^2 = 0.3451$; Fig. 6f). BLI measurements were more sensitive in detecting islets transplanted beneath the renal capsule than into the liver; this technique could consistently detect 25 islets beneath the renal capsule and 100 islets in the liver.

Discussion

This manuscript describes the generation, characterization, and application of a new transgenic mouse line in which luciferase-expressing β cells can be imaged and quantified non-invasively using bioluminescence imaging. Attractive features of the MIP-Luc-VU model are: (1) photon emission from β cells is strong and reproducible and can be detected non-invasively and repeatedly in the same animal. (2) BLI in MIP-Luc-VU mice accurately quantifies changes in β cell mass when this is increased (high-fat feeding) or decreased (streptozotocin treatment). (3) BLI of MIP-Luc-VU islets transplanted beneath the renal capsule or into the liver correlates with the number of islets transplanted and insulin content of the islet graft and persists for more than a year. BLI using the MIP-Luc-VU mouse model builds upon previous work using adenovirus-mediated expression of luciferase in islets and has advantages over two other transgenic lines expressing luciferase in β cells that were reported while this model was under development [30, 31]. The current studies provide an important validation and application of BLI and the MIP-Luc-VU transgenic line and should enhance experimental approaches by providing an accurate, non-invasive assessment of β cell mass.

Validation and application of the MIP-Luc-VU line in the current report represents a significant improvement over adenovirus-mediated luciferase expression since *in vitro* labeling is not needed for the MIP-Luc-VU model, enabling imaging of native islets in the pancreas in addition to transplanted islets [30–32]. BLI measurements reflect the increased β cell mass following β cell proliferation. Furthermore, bioluminescence emission from MIP-Luc-VU islets arises from the β cells, rather than all islet cells, with a small minority (less than 1%) of luciferase-expressing islet cells not expressing insulin. The relative scarcity of these luciferase-expressing, insulin-negative cells indicates that their effect on BLI is negligible. The level of luciferase expression was consistent between animals and after STZ treatment, indicating that BLI can be used to track changes in β cell mass by assaying a representative sample of the total β cell population.

An important caveat about optical imaging is the attenuation of light as it propagates from a point source through tissue before reaching the detector or camera. For example, the site of islet transplantation influences BLI measurements: light emission from islets transplanted into the liver is attenuated more than islets beneath the kidney capsule [30]. In the current study, the obesity in mice fed a high-fat diet attenuated light emission from the pancreas. As previously demonstrated, this light attenuation can be accounted for using a constant light-emitting standard [30]. In the current report, we also used bioluminescence tomographic methods to reconstruct the location of luminescent sources. Even though the spatial resolution of BLI tomography is still less than MRI or PET [44, 45], BLI is currently attractive since the critical need is for quantification of islet mass, not for imaging individual islets.

Several imaging modalities other than BLI are under development for pancreatic islet imaging. For example, approaches that use PET radionuclides [20–22] to label islets *in vitro* are useful for studies of transplanted islets. Targeted PET agents, such as the recently reported studies using radiolabeled dihydrotetrabenazine, may also prove useful in pancreatic islet imaging [27]. MRI has been used to image transplanted islets after “loading” with an MRI contrast agent *in vitro* [13–19, 46, 47]. In contrast with these modalities, bioluminescence imaging has lower cost, higher throughput, and provides quantifiable data

with inherently low background. However, the depth limitation of bioluminescence imaging is on the order of centimeters, precluding clinical application and studies in larger animal models.

Bioluminescence measurements can be influenced by extracellular glucose. In this report and in the two other published reports describing similar transgenic models, light emission from isolated islets cultured overnight in increased glucose *in vitro* was greater [34, 35]. However, neither isolated islets nor animals acutely exposed to high glucose had increased bioluminescence emission. Our studies using an STZ-induced model of diabetes indicate that blood glucose level may also influence BLI *in vivo*. Following STZ treatment, both beta cell mass and BLI were dramatically reduced suggesting that large reductions in β cell mass are accompanied by large reductions in BLI. However, the decline in BLI was slightly less than the decrease in β cell mass (78% versus 96%), suggesting that BLI may be increased by chronic hyperglycemia. Possible mechanisms of how glucose alters cellular bioluminescence may relate to how photons are generated by the bioluminescence reaction involving the enzyme luciferase, the substrate luciferin, and the co-factors, oxygen, ATP, and Mg++ [48]. Since an increase in extracellular glucose leads to increased intracel-lular glucose, increased glucose metabolism, and ATP generation, bioluminescence could be influenced by ATP levels within the β cell, but acute elevations in extracellular glucose during an intraperitoneal glucose tolerance testing did not alter BLI. The proportion of β cells expressing luciferase before and after STZ treatment was similar, indicating that luciferase expression does not influence β cell sensitivity to STZ. The most likely explanations are glucose-regulated transcription of the insulin promoter fragment used to direct transgene expression or glucose-regulated effects on translation on the luciferase mRNA or protein [49]. An attempt to use an alternative promoter fragment to direct luciferase expression to islet cells (fragment of the *pdx1* promoter) was not successful as luciferase was also expressed in other tissues. The practical implication of the effect of glucose on BLI is that while bioluminescence measurements accurately reflect β cell mass in normoglycemic animals, BLI may be increased by modest elevations in the blood glucose. Additional work is needed to define the relationship between the blood glucose and BLI. These studies will need to consider that chronic hyperglycemia leads to beta cell loss and reduced beta cell mass (“glucotoxicity”) so that the beta cell mass may be changing during the experiment. Following this initial characterization of the MIP-Luc-VU model, additional work is needed to determine the relationship between β cell mass and BLI at different blood glucose levels.

Based on the current report, BLI of the MIP-Luc-VU mice should be applicable to a variety of studies that would benefit from non-invasive assessment of β cell mass. These include pre-clinical efforts to increase islet mass, to stimulate β cell regeneration, and to delay β cell loss in models of type 1 and type 2 diabetes. For example, BLI may help elucidate the dynamics of β cell loss in autoimmune models of diabetes such as the NOD mouse (backcrossing of the MIP-Luc-VU transgene onto the NOD background and the ob/ob background is underway). Efforts to increase β cell mass after intrahepatic transplantation should also be facilitated since BLI enables monitoring of changes in β cell mass in the liver.

Supplementary Material

Refer to Web version on PubMed Central for supplementary material.

Acknowledgments

The MIP promoter fragment was graciously provided by Mark Magnuson at Vanderbilt University and the mice were generated in the Vanderbilt Transgenic Mouse/ESC Shared Resource. This study was supported by a grant from the Juvenile Diabetes Research Foundation International, a Merit Review Award from the VA Research

Service, the National Institutes of Health (DK68764, DK66636, DK69603, DK63439, DK62641, DK068751, T35DK07383, T32EB001628), the Vanderbilt Mouse Metabolic Phenotyping Center (DK59637), and the Vanderbilt Diabetes Research and Training Center (DK20593). Work performed in the Vanderbilt University Institute of Imaging Science was supported by SAIRP U24 CA126588.

Abbreviations

MIP	Mouse insulin promoter
Luc	Luciferase
MIP-Luc-VU	Mouse insulin promoter-luciferase-Vanderbilt University
MRI	Magnetic resonance imaging
PET	Positron emission tomography
BLI	Bioluminescence imaging
pdx1	Pancreatic-duodenal homeobox factor-1
NOD-scid	non-obese diabetic-severe combined immunodeficiency
FVB	Friend leukemia Virus B strain
IBMX	Isobutyl methyl xanthine
STZ	Streptozotocin
ROI	Region of interest
PBS	Phosphate-buffered saline
FBS	Fetal bovine serum

References

1. Robertson RP. Islet transplantation as a treatment for diabetes—a work in progress. N Engl J Med (USA). 2004; 350:694–705.
2. Shapiro AM, Lakey JR, Ryan EA, et al. Islet transplantation in seven patients with type 1 diabetes mellitus using a glucocorticoid-free immunosuppressive regimen. N Engl J Med (USA). 2000; 343:230–238.
3. McCulloch DK, Koerker DJ, Kahn SE, Bonner-Weir S, Palmer JP. Correlations of *in vivo* beta-cell function tests with beta-cell mass and pancreatic insulin content in streptozocin-administered baboons. Diabetes (USA). 1991; 40:673–679.
4. Davalli AM, Ogawa Y, Scaglia L, et al. Function, mass, and replication of porcine and rat islets transplanted into diabetic nude mice. Diabetes (USA). 1995; 44:104–111.
5. Davalli AM, Ogawa Y, Ricordi C, et al. A selective decrease in the beta cell mass of human islets transplanted into diabetic nude mice. Transplantation (USA). 1995; 59:817–820.
6. Larsen MO, Rolin B, Wilken M, Carr RD, Gotfredsen CF. Measurements of insulin secretory capacity and glucose tolerance to predict pancreatic beta-cell mass *in vivo* in the nicotinamide/ streptozo-tocin Gottingen minipig, a model of moderate insulin deficiency and diabetes. Diabetes (USA). 2003; 52:118–123.
7. Kjems LL, Kirby BM, Welsh EM, et al. Decrease in beta-cell mass leads to impaired pulsatile insulin secretion, reduced postprandial hepatic insulin clearance, and relative hyperglucagonemia in the minipig. Diabetes (USA). 2001; 50:2001–2012.
8. Saito K, Yaginuma N, Takahashi T. Differential volumetry of A, B and D cells in the pancreatic islets of diabetic and nondiabetic subjects. Tohoku J Exp Med (USA). 1979; 129:273–283.
9. Bonner-Weir S, Trent DF, Weir GC. Partial pancreatectomy in the rat and subsequent defect in glucose-induced insulin release. J Clin Invest (USA). 1983; 71:1544–1553.

10. Virostko J, Jansen ED, Powers AC. Current status of imaging pancreatic islets. Curr Diab Rep (USA). 2006; 6:328–332.
11. Lacy PE. The pancreatic beta cell. Structure and function. N Engl J Med (USA). 1967; 276:187–195.
12. Paty BW, Bonner-Weir S, Laughlin MR, McEwan AJ, Shapiro AM. Toward development of imaging modalities for islets after transplantation: insights from the National Institutes of Health Workshop on Beta Cell Imaging. Transplantation (USA). 2004; 77:1133–1137.
13. Barnett BP, Arepally A, Karmarkar PV, et al. Magnetic resonance-guided, real-time targeted delivery and imaging of magneto-capsules immunoprotecting pancreatic islet cells. Nat Med (USA). 2007; 13:986–991.
14. Biancone L, Crich SG, Cantaluppi V, et al. Magnetic resonance imaging of gadolinium-labeled pancreatic islets for experimental transplantation. NMR Biomed (USA). 2007; 20:40–48.
15. Evgenov NV, Medarova Z, Dai G, Bonner-Weir S, Moore A. *In vivo* imaging of islet transplantation. Nat Med (USA). 2006; 12:144–148.
16. Gimi B, Leoni L, Oberholzer J, et al. Functional MR micro-imaging of pancreatic beta-cell activation. Cell Transplant (USA). 2006; 15:195–203.
17. Jirak D, Kriz J, Herynek V, et al. MRI of transplanted pancreatic islets. Magn Reson Med (USA). 2004; 52:1228–1233.
18. Tai JH, Foster P, Rosales A, et al. Imaging islets labeled with magnetic nanoparticles at 1.5 Tesla. Diabetes (USA). 2006; 55:2931–2938.
19. Zheng Q, Dai H, Merritt ME, et al. A new class of macrocyclic lanthanide complexes for cell labeling and magnetic resonance imaging applications. J Am Chem Soc (USA). 2005; 127:16178–16188.
20. Lu Y, Dang H, Middleton B, et al. Noninvasive imaging of islet grafts using positron-emission tomography. Proc Natl Acad Sci U S A (USA). 2006; 103:11294–11299.
21. Toso C, Zaidi H, Morel P, et al. Positron-emission tomography imaging of early events after transplantation of islets of Langerhans. Transplantation (USA). 2005; 79:353–355.
22. Kim SJ, Doudet DJ, Studenov AR, et al. Quantitative micro positron emission tomography (PET) imaging for the *in vivo* determination of pancreatic islet graft survival. Nat Med (USA). 2006; 12:1423–1428.
23. Clark PB, Gage HD, Brown-Proctor C, et al. Neurofunctional imaging of the pancreas utilizing the cholinergic PET radioligand [18F] 4-fluorobenzyltrozamicol. Eur J Nucl Med Mol Imaging (USA). 2004; 31:258–260.
24. Moore A, Bonner-Weir S, Weissleder R. Noninvasive *in vivo* measurement of beta-cell mass in mouse model of diabetes. Diabetes (USA). 2001; 50:2231–2236.
25. Ladriere L, Malaisse-Lagae F, Alejandro R, Malaisse WJ. Pancreatic fate of a (125) I-labelled mouse monoclonal antibody directed against pancreatic B-cell surface ganglioside(s) in control and diabetic rats. Cell Biochem Funct (USA). 2001; 19:107–115.
26. Schneider S, Feilen PJ, Schreckenberger M, et al. In vitro and *in vivo* evaluation of novel glibenclamide derivatives as imaging agents for the non-invasive assessment of the pancreatic islet cell mass in animals and humans. Exp Clin Endocrinol Diabetes (USA). 2005; 113:388–395.
27. Souza F, Simpson N, Raffo A, et al. Longitudinal noninvasive PET-based beta cell mass estimates in a spontaneous diabetes rat model. J Clin Invest (USA). 2006; 116:1506–1513.
28. Simpson NR, Souza F, Witkowski P, et al. Visualizing pancreatic beta-cell mass with [11C]DTBZ. Nucl Med Biol (USA). 2006; 33:855–864.
29. Contag CH, Spilman SD, Contag PR, et al. Visualizing gene expression in living mammals using a bioluminescent reporter. Photo-chem Photobiol (USA). 1997; 66:523–531.
30. Virostko J, Chen Z, Fowler M, et al. Factors influencing quantification of *in vivo* bioluminescence imaging: application to assessment of pancreatic islet transplants. Mol Imaging (USA). 2004; 3:333–342.
31. Fowler M, Virostko J, Chen Z, et al. Assessment of pancreatic islet mass after islet transplantation using *in vivo* bioluminescence imaging. Transplantation (USA). 2005; 79:768–776.

32. Lu Y, Dang H, Middleton B, et al. Bioluminescent monitoring of islet graft survival after transplantation. Mol Ther (USA). 2004; 9:428–435.
33. Chen X, Zhang X, Larson CS, Baker MS, Kaufman DB. *In vivo* bioluminescence imaging of transplanted islets and early detection of graft rejection. Transplantation (USA). 2006; 81:1421–1427.
34. Park SY, Wang X, Chen Z, et al. Optical imaging of pancreatic beta cells in living mice expressing a mouse insulin I promoter-firefly luciferase transgene. Genesis (USA). 2005; 43:80–86.
35. Smith SJ, Zhang H, Clermont AO, et al. *In vivo* monitoring of pancreatic beta-cells in a transgenic mouse model. Mol Imaging (USA). 2006:5.
36. Hara M, Wang X, Kawamura T, et al. Transgenic mice with green fluorescent protein-labeled pancreatic beta-cells. Am J Physiol Endo-crinol Metab (USA). 2003; 284:E177–E183.
37. Zhang W, Feng JQ, Harris SE, et al. Rapid *in vivo* functional analysis of transgenes in mice using whole body imaging of luciferase expression. Transgenic Res (USA). 2001; 10:423–434.
38. Gannon M, Gamer LW, Wright CV. Regulatory regions driving developmental and tissue-specific expression of the essential pancreatic gene pdx1. Dev Biol (USA). 2001; 238:185–201.
39. Brissova M, Fowler M, Wiebe P, et al. Intraislet endothelial cells contribute to revascularization of transplanted pancreatic islets. Diabetes (USA). 2004; 53:1318–1325.
40. Wang T, Lacik I, Brissova M, et al. An encapsulation system for the immunoisolation of pancreatic islets. Nat Biotechnol (USA). 1997; 15:358–362.
41. Brissova M, Shiota M, Nicholson WE, et al. Reduction in pancreatic transcription factor PDX-1 impairs glucose-stimulated insulin secretion. J Biol Chem (USA). 2002; 277:11225–11232.
42. Brissova M, Fowler MJ, Nicholson WE, et al. Assessment of human pancreatic islet architecture and composition by laser scanning confocal microscopy. J Histochem Cytochem (USA). 2005; 53:1087–1097.
43. Brissova M, Blaha M, Spear C, et al. Reduced PDX-1 expression impairs islet response to insulin resistance and worsens glucose homeostasis. Am J Physiol Endocrinol Metab (USA). 2005; 288:E707–E714.
44. Virostko J, Powers AC, Jansen ED. Validation of luminescent source reconstruction using single-view spectrally resolved bioluminescence images. Appl Opt (USA). 2007; 46:2540–2547.
45. Kuo C, Coquoz O, Troy TL, Xu H, Rice BW. Three-dimensional reconstruction of *in vivo* bioluminescent sources based on multispectral imaging. J Biomed Opt (USA). 2007; 12:024007.
46. Kriz J, Jirak D, Girman P, et al. Magnetic resonance imaging of pancreatic islets in tolerance and rejection. Transplantation (USA). 2005; 80:1596–1603.
47. Medarova Z, Evgenov NV, Dai G, Bonner-Weir S, Moore A. *In vivo* multimodal imaging of transplanted pancreatic islets. Nat Protoc (USA). 2006; 1:429–435.
48. Kennedy HJ, Pouli AE, Ainscow EK, et al. Glucose generates sub-plasma membrane ATP microdomains in single islet beta-cells. Potential role for strategically located mitochondria. J Biol Chem (USA). 1999; 274:13281–13291.
49. Nielsen DA, Welsh M, Casadaban MJ, Steiner DF. Control of insulin gene expression in pancreatic beta-cells and in an insulin-producing cell line, RIN-5F cells. I. Effects of glucose and cyclic AMP on the transcription of insulin mRNA. J Biol Chem (USA). 1985; 260:13585–13589.

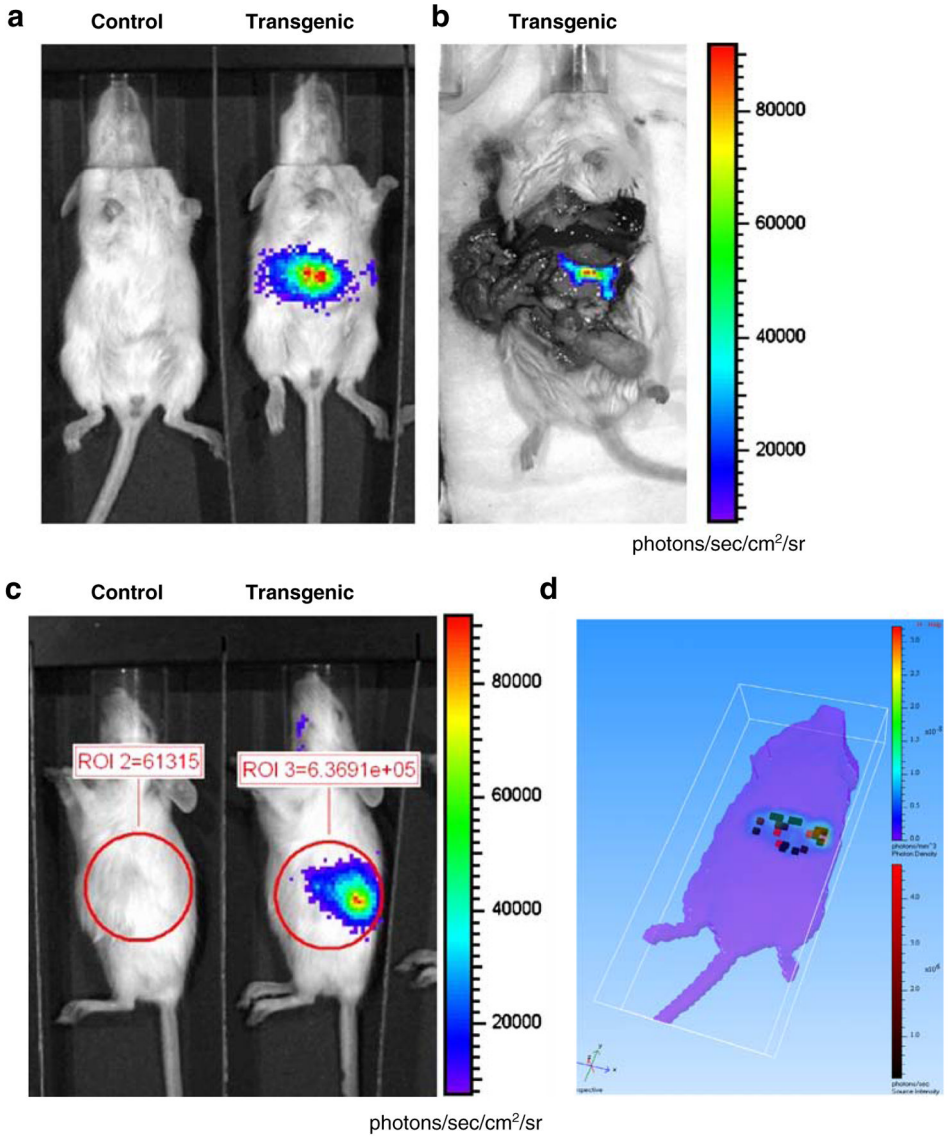

Fig. 1.

In vivo bioluminescence imaging of mice expressing luciferase under control of the mouse insulin I promoter detects light emission from the pancreas. **a** A MIP-Luc-VU transgenic mouse, but not control mouse, emitted light after administration of the luciferin substrate in an anatomical region consistent with the pancreas. **b** After injection of luciferin, the abdominal cavity was immediately opened to expose the pancreas and verify that all light emission was emanating from the pancreas; no other organs emitted light. **c** A MIP-Luc-VU mouse placed in a right lateral decubitis position displayed light emission from the pancreatic region. Regions of interest drawn over the bioluminescent region demonstrate the manner in which bioluminescence emission was quantified. **d** Three-dimensional reconstruction of bioluminescence from the pancreas of a MIP-Luc-VU mouse. Clusters of bioluminescent islets are reconstructed as red voxels within the volume of the mouse. The surface projection from the bioluminescent islets is displayed on the rainbow color scale. BLI in MIP-Luc-VU mice was similar in males and females and between mice of different generations and ages. There was no statistically significant difference between age-matched male and female control mice used in these studies (P=0.199, unpaired t test) used for

subsequent STZ and high-fat diet experiments. The mice used in the STZ experiment and high-fat diet came from successive generations of MIP-Luc-VU mice. There was no significant difference between the STZ control cohort (four mice, approximately 60 islets/mouse) and high-fat control cohort (three mice) as determined by unpaired t test (P=0.5654). The control mice used in the high-fat diet were imaged at 1, 3, and 6 months of age and there was no significant difference in bioluminescence intensity as determined by ANOVA.

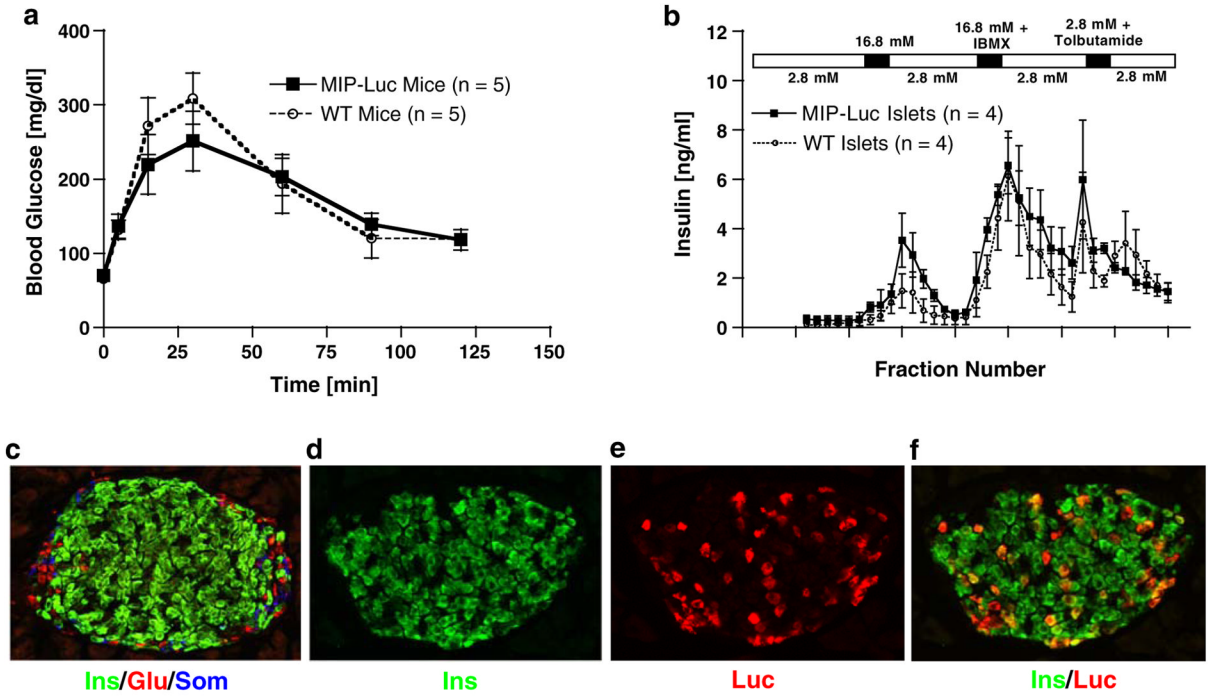

Fig. 2.

MIP-Luc-VU mice have normal glucose tolerance, insulin secretion, and islet morphology. **a** Intraperitoneal glucose tolerance testing of MIP-Luc-VU animals (*black squares*) revealed similar response to a glucose bolus (1.5 g/kg body weight) as wild-type control animals (*open circles; n*=5 each group). **b** Isolated MIP-Luc-VU islets (*black squares*) displayed similar insulin release in response to islet secretagogues as islets isolated from wild-type animals (*open circles*) when tested in a cell perifusion apparatus (*n*=4 each group). The time of exposure to each islet secretagogue (16.8 mM glucose, 16.8 mM glucose+ 100 μM isobutyl methyl xanthine, and 2.8 mM glucose+300 μM tolbutamide) is indicated by the bar above the chart. Immunocytochemistry of MIP-Luc-VU islets stained for insulin (*green*), glucagon (*red*), and somatostatin (*blue*) (**c**); insulin (**d**); luciferase (**e**); and insulin (*green*) and luciferase (*red*) (**f**). This pattern of expression of luciferase was similar in different mice. There was not a significant difference between the number of luciferase-positive beta cells in the STZ control cohort (four mice, approximately 60 islets/mouse) and high-fat control cohort (three mice) as determined by unpaired *t* test (*P*=0.5654)—see Figures 4 and 5.

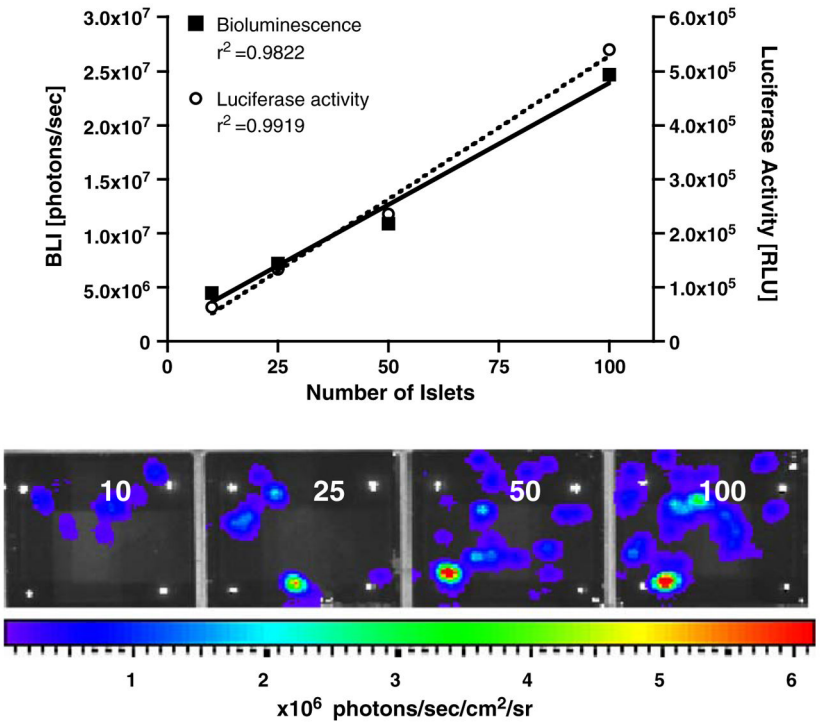

Fig. 3.

Bioluminescence of MIP-Luc-VU islets correlates with the number of islets *in vitro*. Islets in quantities of 10, 25, 50, and 100 islets (*left to right*) were placed in a 24-well plate and *in vitro* bioluminescence imaging was performed after addition of luciferin (*lower panel*). Quantification of *in vitro* bioluminescence (*left y-axis*) reveals linear correlation between bioluminescence intensity and the number of islets (*black squares; upper panel*). Luciferase activity in islet lysates (*right y-axis*), as measured by luminometer, also correlates with the number of islets (*open circles; upper panel*).

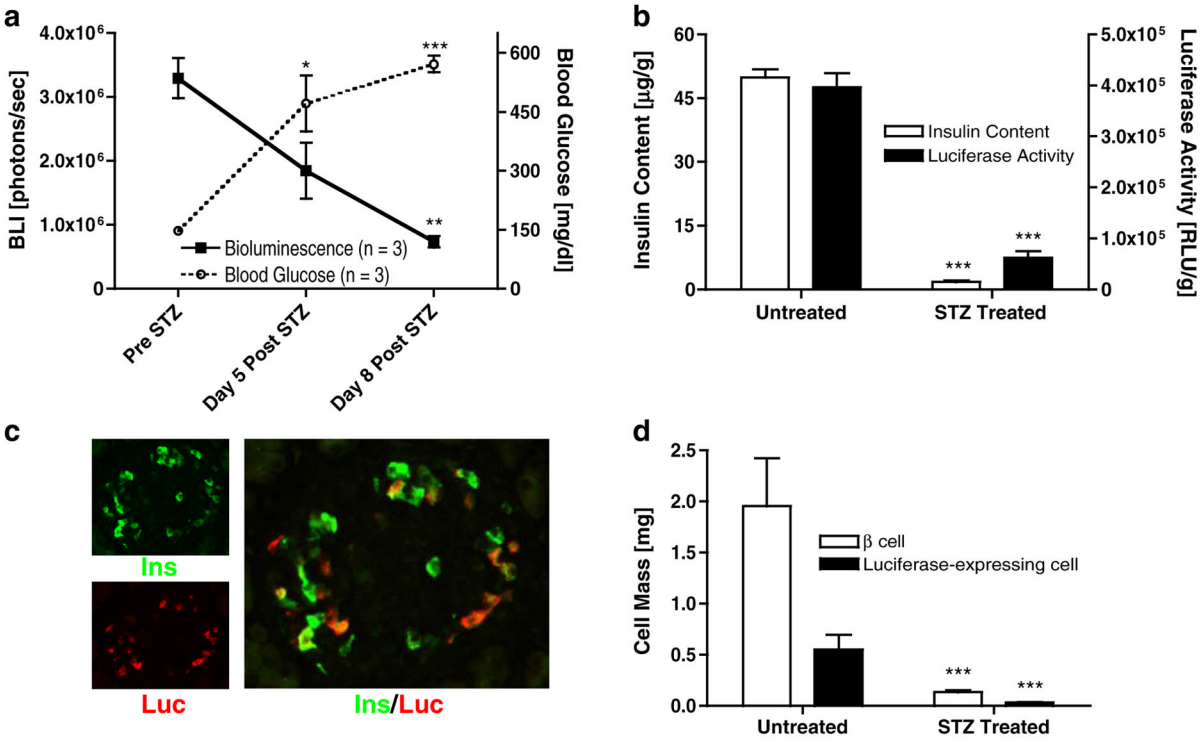

Fig. 4.

BLI declines after β cell destruction and correlates with β cell mass. a Treatment with streptozotocin (STZ, 175 mg/kg) leads to a progressive decline in bioluminescence (*black squares*) from MIP-Luc-VU mice (n=3) and is accompanied by an increase in blood glucose level (*open circles;* n=3). b The insulin content (*white bar*) and luciferase activity (*black bar*) of pancreata excised from untreated control MIP-Luc-VU mice is higher than in mice 8 days after STZ injection (n=4). Luciferase activity and insulin content measurements were performed on separate pancreatic extracts. c Immunocytochemistry of an islet from a MIP-Luc-VU mouse 8 days after STZ treatment was stained for insulin (*green*) and luciferase (*red*). The larger panel shows co-labeling of cells for insulin and luciferase. d The mass of β cells (white bar) and luciferase-expressing cells (*black bar*), as determined by morphometric analysis, of MIP-Luc-VU mice 8 days after STZ administration was significantly reduced compared with untreated control pancreata (n=4 mice, 30–40 islets per mouse; unpaired *t* test; *p<0.05; **p<0.01; ***p<0.005).

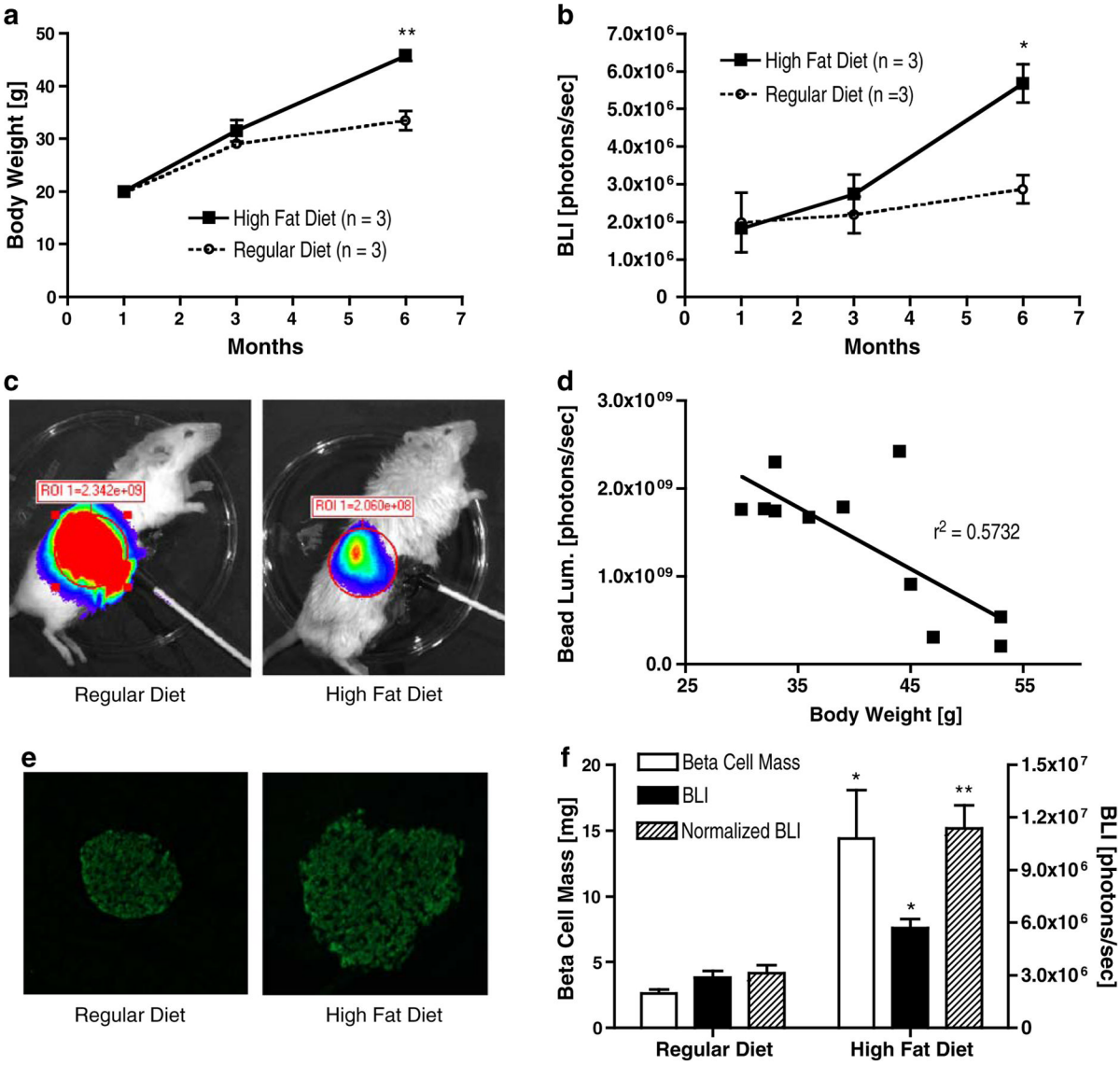

Fig. 5.

BLI correlates with increased β cell mass induced by high-fat feeding. **a** MIP-Luc-VU mice fed a high-fat diet (*black squares*) displayed a progressive increase in body weight as compared with MIP-Luc-VU mice fed a regular diet (*open circles*). **b** Over the same time period MIP-Luc-VU mice fed the high-fat diet (*black squares*) had higher bioluminescence emission than MIP-Luc-VU mice fed a regular diet (*open circles*). **c** Light emission from a luminescent bead implanted at the pancreas was higher for mice fed a regular diet (*left*) than for a mouse fed a high-fat diet (*right*). **d** Correlation between the animal weight and the amount of light detected from a luminescent bead placed at the site of the pancreas. **e** Immunocytochemistry of an islet stained for insulin from mice fed a regular diet (*left*) or high-fat diet (*right*). **f** Morphometric analysis of insulin labeling of islets revealed greater β cell mass in mice fed the high-fat diet (*white bars*), reflected by increased BLI measurements (*black bars*), but more closely correlating with BLI measurements normalized for animal body habitus (*hatched bars*; unpaired *t* test; **p*<0.05; ***p*<0.01; ****p*<0.005).

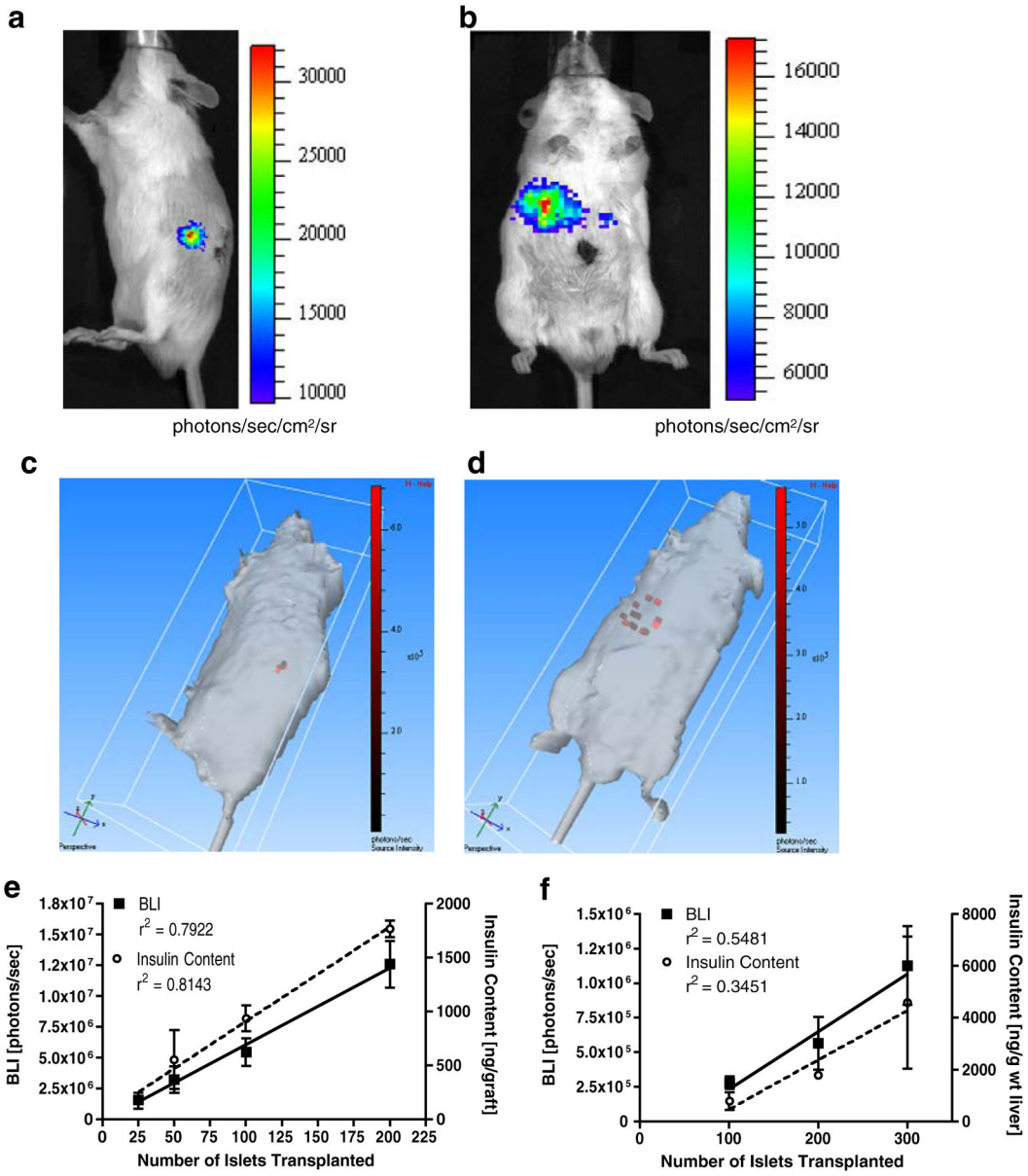

Fig. 6.

MIP-Luc-VU islets can be imaged and their mass assessed *in vivo* after transplantation. MIP-Luc-VU islets were transplanted beneath the kidney capsule (**a**) or into the liver via portal vein infusion (**b**) of NOD-scid mice. **c** Three-dimensional reconstruction of islets beneath the kidney capsule reveals a small, contiguous islet graft within the kidney. Islets are shown as red voxels within the volume of the mouse. **d** Three-dimensional reconstruction of islets infused via the portal vein reveals islets scattered throughout the liver. **e** The number of islets transplanted to the renal capsule correlates linearly with bioluminescence and the insulin content of the graft (n=4). **f** Islets transplanted to the liver display a similar correlation between the number of islets transplanted, bioluminescence, and hepatic insulin content (n=4). The relatively low R2 values in the liver reflect the variability in islet engraftment after portal vein infusion, as indicated by the variability in post-mortem insulin content measurements. The variability in BLI measurements mirrors this inconsistent engraftment of islets in the liver.